8th World Conference on Experimental Heat
Transfer, Fluid Mechanics, and Thermodynamics
June 16-20, 2013, Lisbon, Portugal

# HEAT TRANSFER CHARACTERIZATION OF A SINGLE SOURCE ULTRA-LOW FLOW RATE ELECTROSPRAY

Michael Gibbons[a], Shane Finnegan[b], Michael Maguire[b], Shirley O'Dea[c], Anthony Robinson[a]

[a] Department of Mechanical & Manufacturing Engineering, Trinity College Dublin, Ireland
[b] Profector Life Sciences, NUI Maynooth, Ireland
[c] Institute of Immunology, Biology Department, NUI Maynooth, Ireland
E-mail : migibbon@tcd.ie

## ABSTRACT

The development and optimization of two phase electrospray cooling is currently restricted, in part due to the insufficient knowledge of how the various parameters that define an electrospray interact and their subsequent effect on the heat transfer coefficients and profiles. This research aims to characterise the heat transfer to impinging electrosprays for different nozzle sizes, separation heights and flow rates. The results show that electrospray cooling is dependent on separation height and cooling fluid flow rate, and partially on nozzle size. At lower separation heights and greater flow rates a *saturation point* was observed where a subsequent increase in the flow rate yields no increase in the peak heat transfer coefficient. In the case of greater separation heights and lower flow rates a *dispersion threshold* was noted where the working fluid becomes too dispersed causing reduced heat transfer coefficients. The radial enhancement region was shown to be slightly sensitive to varying flow rate and separation height though independent of nozzle size. Nozzle size was found to be important for moderate separation heights and high flow rates. Importantly, the results show that very high peak heat transfer enhancement over natural convection can be achieved with electrosprays with exceptionally low flow rates.

**Keywords**: Electrospray, Spray cooling, Electronic cooling, Thermal management

## 1. INTRODUCTION

As modern day electronics becomes more densely packed with transistors, the technology sector finds itself fast approaching a thermal management threshold, where conventional cooling technologies will be unable to effectively meet the needs of the aggressively advancing electronics industry. Conventional fan cooling or natural convection has been widely applied as the standard method of thermal energy dissipation for industrial and consumer electronics given their simplicity and robustness. However these are no longer considered a sustainable solution given the continued accelerated advancements made within the electronics industry. Effective thermal energy dissipation is crucial in maintaining a products performance and life cycle.

An emerging solution to this thermal management problem is electrospray cooling (EC). In order to dissipate higher heat fluxes from advanced microelectronics utilization of phase change cooling technologies, such as electrospray cooling, show great promise.

EC utilises Coulomb forces for energy efficient fluid atomization. Fine liquid droplets are propelled from the nozzle to the target by a potential difference that exists between the source and target. The required voltage potential to induce electrospraying is dependent on the cooling fluid properties and the mode of spraying being implemented with very low additional energy requirements [1, 2]. By altering certain parameters one can precisely control droplet size, distribution and associated heat transfer.

Electrospraying is an attractive proposition for cooling applications because they offer low profile liquid cooling performance with extremely low liquid flow rates, they do not require compressed air to generate the atomized spray and do not entail any significant additional electrical power to operate. This would make EC technology particularly attractive for space application, where size and weight restrictions are vital and there are no buoyancy forces for natural convection. Unlike conventional sprays, EC also enables almost complete avoidance of rebound losses, which reduce spray efficiency, as a result of the Coulombic attraction that exists between the charged coolant and the target [3].

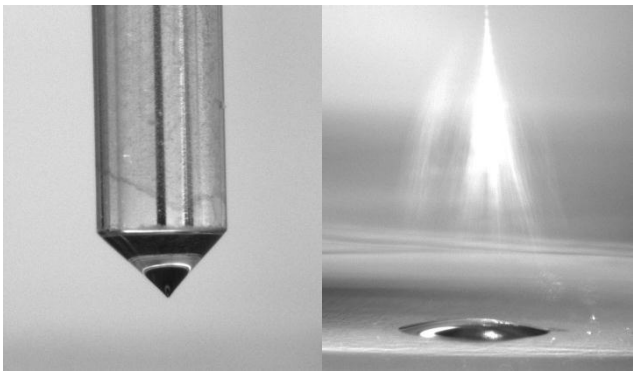

**Fig. 1**. Electrospray cooling cone-jet mode, (left) Taylor cone, (right) spray plume

### 1.1 Research objectives

Initial research [4-7] has shown that EC technology is a viable option as a thermal management solution for small form factor electronics. Feng and Bryan [4] were the first to investigate two phase electrospray cooling. During their research they studied the heat transfer characteristics of two-phase

impinging liquid cooling for different capillary tube arrays in an enclosed chamber. Their work showed that optimum heat transfer enhancement existed at lower heat fluxes (less than 30 W/cm$^2$). This condition corresponded to the ramified jet regime of spraying and resulted with an enhancement of 1.7 times over natural convection alone.

Wang and Mamishev [6, 7] built on the work by Feng and Bryan by exploring the interaction of nozzle spacing and the subsequent effect on the averaged heat transfer coefficient. A peak enhancement ratio of 1.87 was achieved for an 8 nozzle, 5mm spacing array at the lowest heat flux. In their follow on research they developed multiple Nusselt number correlations for different geometric nozzle spacing and arrangements. The correlations they developed covered over 83% of the experimental data with a ± 10% deviation.

Deng and Gomez [5] demonstrated microfabricated multiple source arrays. An optimal average heat flux removal of 96 W/cm$^2$ with a cooling efficiency of 97% was achieved for the designed system.

Unlike past research highlighted above, all of which focused on the averaged heat transfer coefficient for the electrospray cooling, this research endeavors to investigate the local heat transfer achievable by a single nozzle electrospray in the cone-jet mode regime under evaporative cooling conditions. Specifically, ultra-low flow rates are studied. This was achieved using an ohmically heated thin foil and thermal imaging system in order to fully investigate and characterise the local cooling features of the electrospray under varied operating parameters.

## 2. BACKGROUND

In 1917 John Zeleny [1] first observed that the nature of liquid dipping and sprays changed under application of an electric field. It was not until 1964 that Geoffrey Taylor [8] provided a theoretical explanation for the "Taylor" cone-jet mode that Zeleny observed (Fig. 1) [2, 6].

When a voltage is applied a nozzle an electric field is created between the source and the target surface. This applied voltage induces charges within the working fluid. As the voltage is increased the electric field and the charge density also increases. At a critical voltage the induced Coulomb forces act on the charges in the working fluid resulting in the meniscus deforming into the shape of a cone (Fig. 1). This cone is extended at its apex by a permanent jet which breaks into a stream of charged droplets to form a spray. These charged droplets repel each other causing drop dispersion i.e. spreading of the jet spray, and are then accelerated towards the target thermal exchange surface due to electrostatic forces [2]. If the applied voltage continues to increase a multi-jet mode of spraying will be induced [2, 9].

While the multi-jet mode enables greater surface area coverage, the droplets generated are of a poor consistency [7] and the cone creation and position on the nozzle are unpredictable. The cone jet mode in contrast is particularly appealing due to its stability, predictability and fine droplet creation [2].

## 3 EXPERIMENTAL SETUP

### 3.1 Experimental Apparatus

The experimental apparatus is shown in Fig. 2 and Fig. **3**. A schematic of the rig design can be seen in Fig. 4 for further clarification.

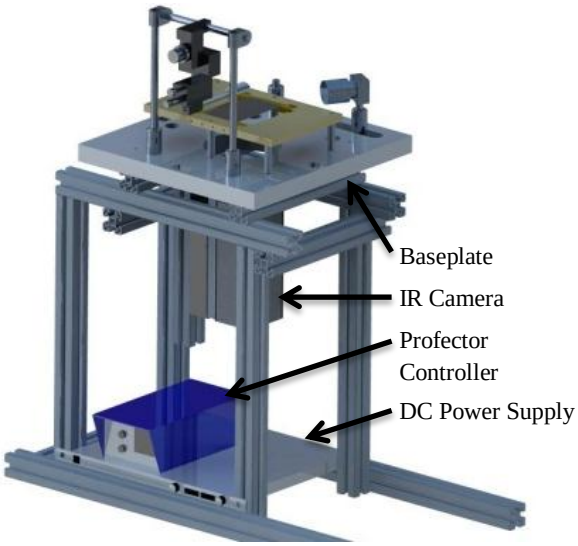


**Fig. 2.** Electrospray test cell

#### 3.1.1 Electrospray System

Both the applied nozzle voltage and flow rate were supplied by a Profector Life Sciences Electrospray Controller (Fig. 2. Electrospray test cell The voltage potential and flow rate ranged between 2kV to 5.5kV and 1 – 16 µl/min respectively during experimentation. The controller utilized a backpressure system to set the desired flow rates for the working fluid. Backpressure was chosen as opposed to the widely used syringe pump as it enabled a steady flow rate in contrast to the pulsed flow induced by typical screw controlled syringe pumps at these low flow rates.

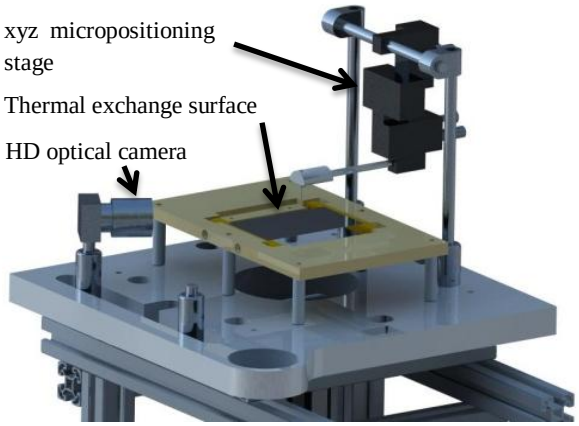


**Fig. 3.** Electrospray baseplate

A micropositioning xyz optical stage (Fig. 3) was used to control the separation height, H, between the source nozzle and the thermal exchange target surface. The height was varied from

a minimum of 2.5 mm in 2.5 mm increments up to 12.5 mm. Five nozzle sizes were characterised; d = 0.108 mm, 0.180 mm, 0.330 mm, 0.712 mm and 1.066 mm over the course of the experimentation. These separation heights and nozzle sizes were chosen in order to investigate electrospray cooling over a wide range of performance criteria.

### 3.1.2 Heated Foil and Surrounding Structure

The baseplate (Fig. 2) is constructed from Delrin plastic of dimensions 400mm x 320mm x 30mm and is supported by an aluminium profile frame. The target surface (Fig. 3) consists of a 275mm x 180mm x 11mm polyrtheretheketone (PEEK) housing and the ohmically heated foil. The heated foil measures 115mm x 70mm x 25µm and is bonded between two copper bus bars using electrically conductive epoxy.

Each bus bar has two connections on each end to which DC current was supplied from a DC power supply. The power supply has the capability of providing 8 volts and 100 amps in either constant voltage or constant current modes. The copper bus bars are mounted to the PEEK structure. PEEK was chosen given its high temperature performance characteristic (>200$^0$C).

One set of bus bars is rigidly fixed to the PEEK while the others are spring loaded and serve the purpose of tensioning the foil. After the foil was cured, the springs were adjusted to tension the foil. This tensioning system ensured that the foil remained taut for varying wall heat fluxes. The underside of the foil was exposed for direct temperature measurement by the infrared camera. To facilitate accurate temperature measurement, the exposed underside area of the foil was coated with a thin layer of matt black paint with an emissivity ε = 0.9 so as to minimize the effects of reflection and provide a surface of known emissivity

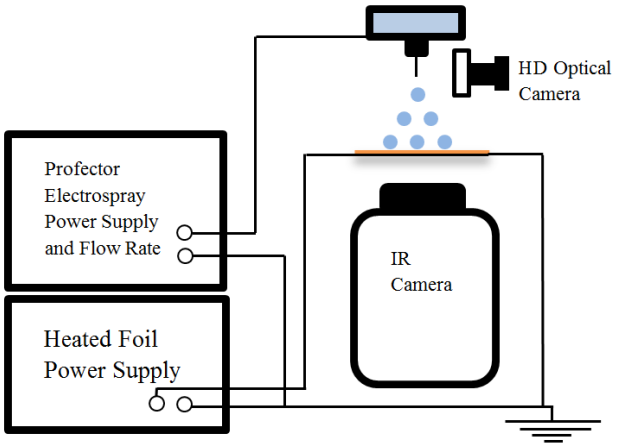


**Fig. 4.** Experimental Rig Schematic

### 3.1.3 Imaging System

The imaging system consisted of two parts; a high definition optical camera and a thermal imaging camera. The optical camera was used to focus on the nozzle tip and to define when the cone-jet regime of spraying had been induced.

To capture and record the thermal footprint created by the electrospray, a FLIR A-40 camera and the ThermaCAM Researcher PRO 2.9 software were operated in tandem. The total camera viewing area was 15.2 mm by 11.4 mm with a spatial resolution of 47.5 µm and a frame rate up to 50 Hz. The camera was mounted to the aluminium profile frame (Fig. 2) directly below the thermal exchange test surface. At each data point, 3 sets of 500 images at 50Hz were recorded. These sets were taken at one minute intervals and were initialized only after steady state conditions were reached. All recorded results were processed using Matlab.

### 3.1.4 Working Fluid

All tests were conducted with 100% ethanol, with a boiling point of 78.37$^0$C. Ethanol was chosen given its favourable fluid characteristics. Its low surface tension enables the onset of cone jet regime electrospraying at relatively low applied voltages. Ethanol also possesses favorable electrical conductivity enabling stable spraying by ensuring the electric forces are much stronger than the intermolecular forces within the fluid.

Water and other fluids with greater surface tension characteristics are not suitable for the purpose of electrospraying as the voltage potential required to implement the spraying of the liquid is close to that of the electrical coronal discharge of air under atmospheric conditions [1].

All experiments were conducted at atmospheric pressure and room temperature after steady state conditions were reached. The thermal exchange surface temperature was assumed to be uniform across its thickness and was maintained at a constant heat flux input of 1,082.6 W/m$^2$ for all test points. Given the thickness of the foil (25µm), the conductive thermal resistance through the thickness is assumed negligible such that the temperature on the top of the foil is equal to that at the bottom (see biot number consideration below). Lateral conduction within the foil was shown to be negligible using a Finite Element model created using COMSOL Multiphysics 4.3.

## 4. RESULTS AND DISCUSSION

### 4.1 Equations and units

The heat transfer coefficient was calculated using the expression:

$$h = q" / \Delta T \quad (1)$$

where ΔT is the temperature difference between the foil and that of the fluid temperature. $q"$ is the heat flux and is assumed uniform across the thermal exchange surface since lateral conduction was negligible. It is determined from the current passing through the foil, I, the resistivity of the foil, R, under testing conditions and the surface area, $A_s$, of the thermal exchange surface.

$$q" = I^2R/A_s \quad (2)$$

In analyzing the recorded results an energy balance was implemented at each node on the thermal exchange surface and is given by:

$$q"_{EC} = q"_{Gen} - q"_{Rad,total} - q"_{Conv} \quad (3)$$

where $q"_{EC}$ is the heat dissipated by the electrospray cooling, $q"_{Gen}$ is the heat generated, $q"_{Rad,total}$ is the radiation from the top and bottom sides of the foil and, $q"_{Conv}$ is the thermal energy dissipated by natural convection from the bottom surface. As the electrospray is axisymmetric about its nozzle centre, one can consider the concept of a radial heat transfer enhancement region. The region is measured as a distance radially outward from the projected centre of the nozzle. This area of enhancement can be defined as the region where a minimum 5% increase in local wall heat transfer compared to the no-spray, natural convection case. The enhancement radius is then calculated as,

$$R_{enhancement} = r_{@1.05q"NC} \quad (4)$$

The electric field can be calculated by approximating it as the field between a hyperboloid and plate [4, 10]

$$E_0 = 4V/(D_0 \ln(8H/D_0)) \quad (5)$$

where V is the applied voltage to the nozzle source to induce the Taylor cone, $D_0$ is the outer diameter of the source nozzle, H is the separation distance of the source nozzle to the thermal exchange surface.

The Biot number, Bi, is used in demonstrating that the conductive thermal resistance through the thickness of the foil is negligible. This condition can be considered true if Bi < 0.1, where the Biot number is given by

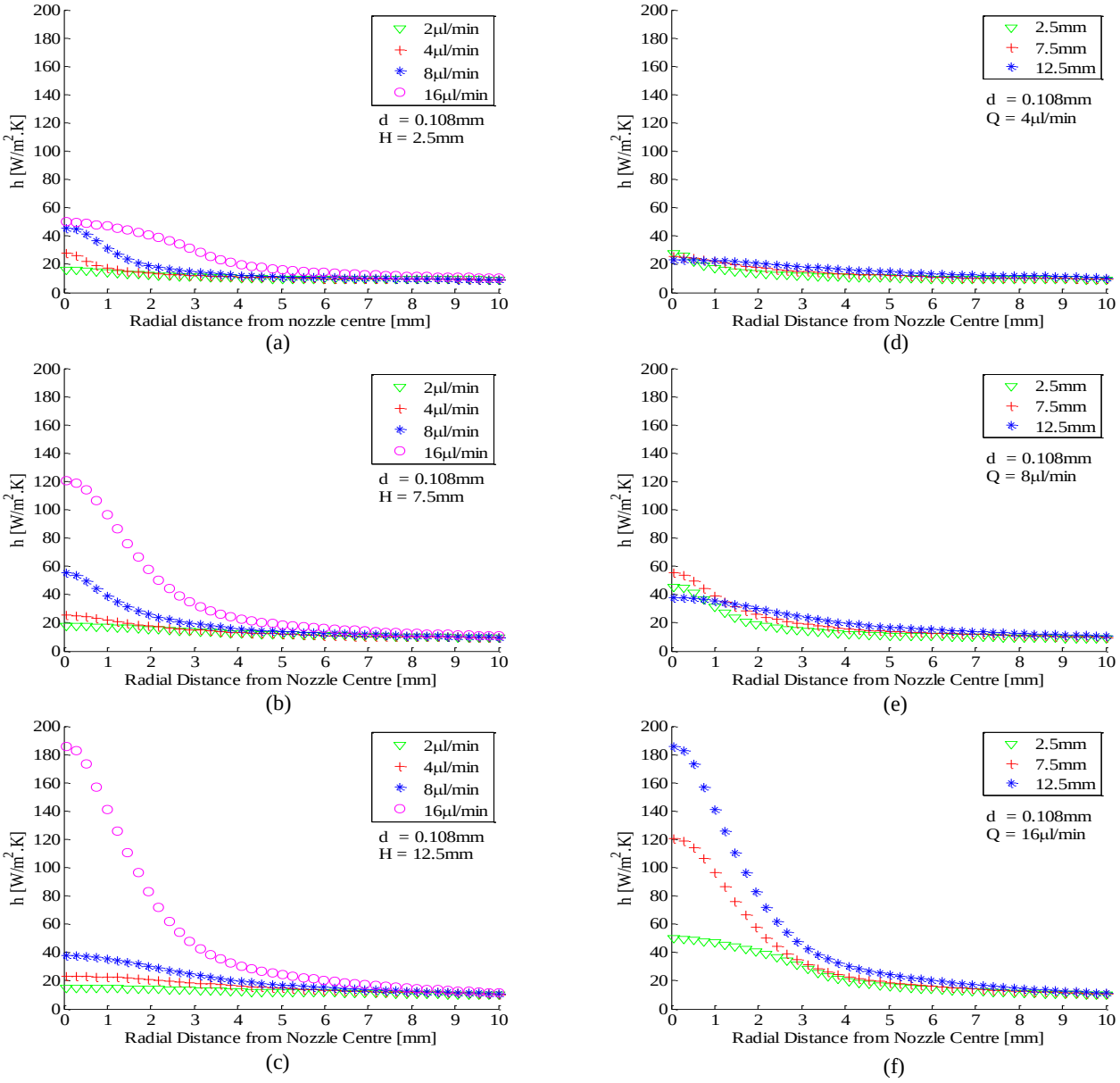


**Fig. 5.** Heat transfer coefficient profiles for a 0.108mm nozzle at constant foil input heat flux of 1,082.6 W/m$^{2:}$ (a) – (c) depict set distances to target, H, for increasing flow rates, Q; (d) – (f) show set flow rates with increasing distances to target

$$Bi = hL_c/k$$

where h is the highest heat transfer coefficient observed, $L_c$ is the characteristic length ($volume_{foil}$/surface $area_{foil}$) and k (16.3 W/mK) is the thermal conductivity of the foil. Using a $h_{max}$ of 400 W/m$^2$K we derive bi ≈ 3.067x10$^{-}$3 which << 0.1.

### 4.2 Heat Transfer Coefficient Results

#### 4.2.1 Effect of Flow Rate and Nozzle Height for d=0.108mm

Fig. 5 consists of six plots demonstrating the effect that the working fluid flow rate, Q, and the separations height, H, has on the heat transfer coefficient profiles for the d = 0.108 mm nozzle. Plots (a) - (c) are for H = 2.5mm, 7.5mm and 12.5mm respectively. Each plot shows the influence of volumetric flow rate ranging between 2 µl/min ≤ Q ≤ 16 µl/min.

For a given separation height and nozzle size, it was observed that an increase in flow rate results in a subsequent increase in the magnitude and spread of the heat transfer coefficient. This can be seen to the greatest extent in the H = 12.5 mm separation test (Fig. 5(c)). For the H = 2.5 mm case at Q = 16 µl/min it was observed that there was considerable pooling of the cooling fluid in comparison with the 7.5 mm and 12.5 mm conditions. This is caused by the increased flow rate and the reduced separation height between source and thermal exchange surface. The finely created droplets do not have sufficient separation distance to establish effective plume dispersal. As a result of this pooling, similar peak heat transfer coefficients are observed for both the 8 µl/min and 16 µl/min tests, although for the 16 µl/min case a broad region of almost uniform heat transfer coefficient can be seen near r = 0mm. From this result one can conclude that there exists a *saturation point* where subsequent increase in fluid deposition will not affect the maximum heat transfer coefficient, though it will alter the cooling profile. This *saturation point* is dependent on the separation height, flow rate and target surface temperature.

The second group of plots, Fig. 5(d) - (f), correspond to a constant flow rate and nozzle size for varied separation heights. Each plot corresponds to an increasing flow rate from Q = 4 µl/min to Q = 16 µl/min. Plots (d) and (e) show that for lower flow rates and greater separation height (H = 12.5 mm) a larger region of uniform cooling is achieved but the peak heat transfer coefficient is lower. For smaller separation heights a more confined region of peak heat transfer coefficient is observed. This trend does not hold consistent though for Q = 16 µl/min. Here it is observed that both the peak heat transfer coefficient and the spread improve as the separation height increases. This can be attributed to a *dispersal threshold*. As the separation height increase the electrostatically induced droplets have greater time over which to repel each other which causes greater plume dispersion for increasing levels of H. At lower flow rates and greater separation heights the plume becomes too dispersed resulting in the finely created droplets evaporating before contacting the thermal exchange surface, which is maintained above the working fluids boiling point. This fact can be more clearly conveyed through examination of Fig. 6.

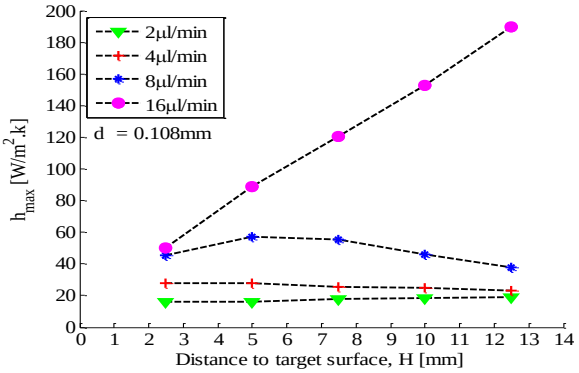


**Fig. 6.** Heat transfer coefficient of a 0.108mm source for increasing source heights with increasing working fluid flow rates

Fig. 6 compares the peak heat transfer coefficient, $h_{max}$, with source to target separation height for varying flow rates. The plot demonstrates clearly the aforementioned *dispersal threshold*. As the height increases a point is reached where maximum peak heat transfer is realized. For the 2 µl/min and 4 µl/min flow rates the peak heat transfer coefficient is not very sensitive to H and thus the location of the maximum is difficult to judge and may in fact be lower than the minimum separation height tested. The 8 µl/min case shows a distinct maximum value for the peak heat

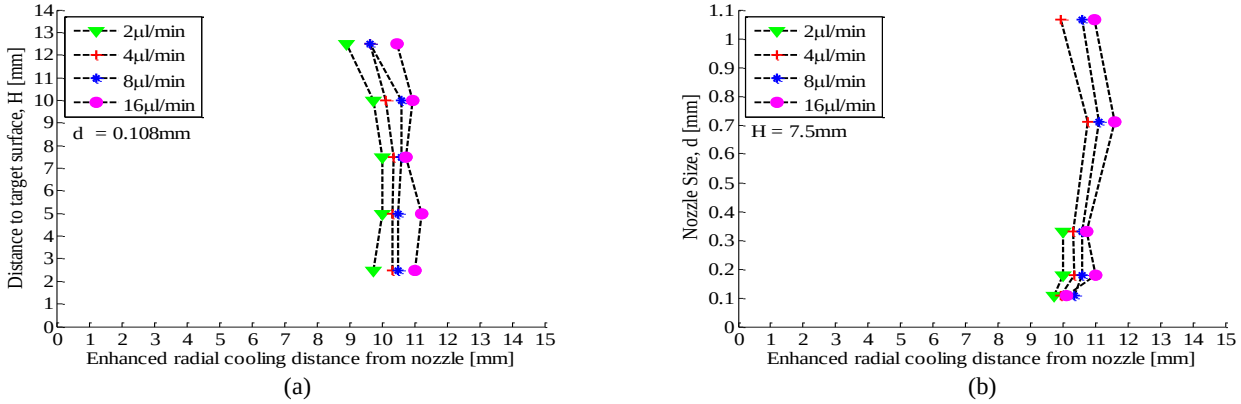


**Fig. 7.** Comparison on effect of distance to target and source nozzle size for increasing working fluid flow rates for a set foil input heat flux of 1,082.6 W/m$^2$; (a) source diameter of 0.108mm (b) set distance to target height of 7.5mm

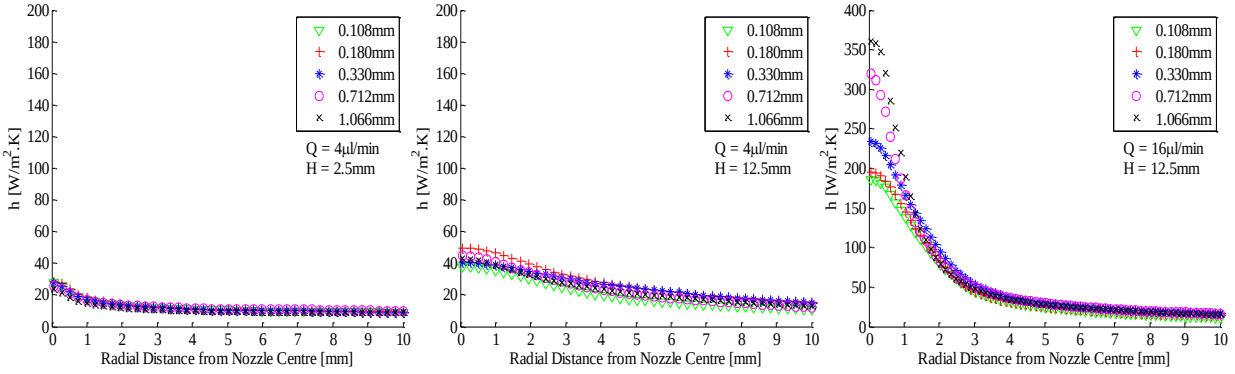


**Fig. 9**

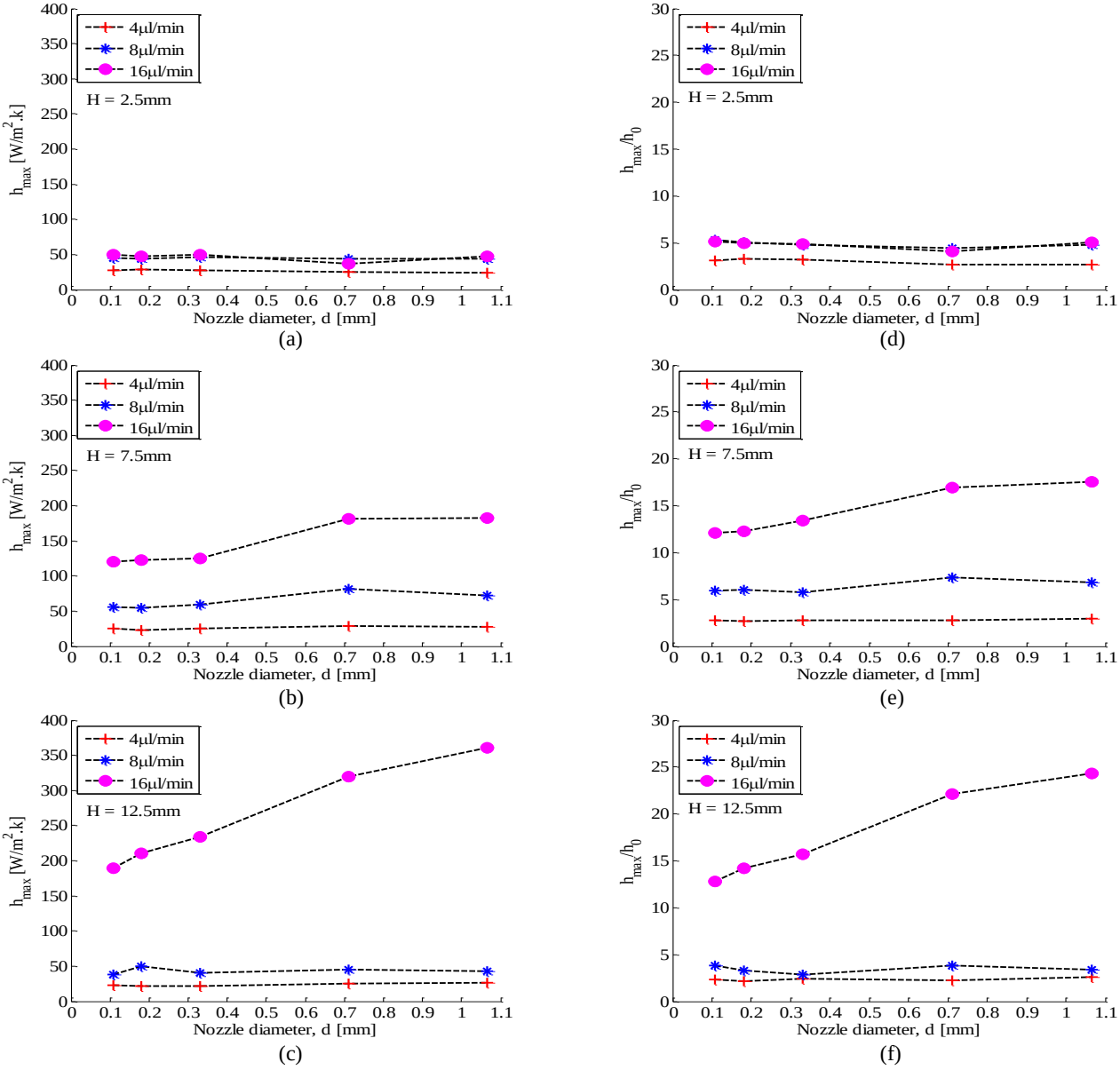


**Fig. 9.** Effect varied source nozzle sizes has on the peak and enhanced heat transfer coefficient for increasing separation height and working fluid flow rates at constant foil input heat flux of 1,082.6 W/m$^2$; (a) – (c) peak heat transfer coefficients, Q, (d) – (f) enhanced heat transfer coefficients

transfer coefficient at approximately H = 5 mm. The peak heat transfer coefficient of the 16 µl/min case continues to increase for increasing separation height without reaching its threshold point. It is hypothesized that this limit would lie beyond the largest H tested. From the results of Fig. 5 and Fig. 6, it can be then deduced that, for a given wall heat flux, an optimum separation height and flow rate may exist to maximise the peak heat transfer coefficient of the electrospray.

Fig. 7 compares the effects that varying the separation height and the source nozzle diameter, d, have on the enhancement radius achieved for increasing flow rates. From Fig. 7(a) it can generally be said that that the enhancement radius decreases marginally with increasing separation height and increases with increasing flow rate. For the latter, an average increase of 12.4% in the enhanced radius is measured for a 700% increase in flow rate. It must be noted however that a small increase in effective radius will have a disproportionately large increase in the effective surface area, which is proportional to the square of the effective radius. As noted, Fig. 7(a) also highlights that, for a fixed flow rate, an increase in separation height results in a marginal 7.14% decrease in the enhancement region. However it is noteworthy to mention that as seen from Fig. 5, while the enhanced region may not be sensitive to H, the area averaged heat transfer coefficient does since the magnitude of the local heat transfer coefficient increases with increasing H.

#### 4.2.1 Effect of Nozzle Diameter

Fig. 9 illustrates the effect that varying the nozzle size has on the radial heat transfer profile. Fig. 9(a) and (b) are of a constant flow rate of Q = 4 µl/min and heights of H = 2.5 mm and H = 12.5 mm respectively. Interestingly, it is observed that the heat transfer coefficient distribution is almost completely independent of the nozzle size implemented. Considering the enhancement radius plots in Fig. 7(b) and the peak heat transfer coefficient plots of Fig. 9(a) it can be said that, for a given flow rate, the nozzle size does not influence the heat transfer at the lowest target spacing of H = 2.5 mm. The same thing can be said for all flow rates tested that are less than or equal to 8 µl/min (Fig. 9(b) & (c)). However, Fig. 9(c), (b) and (c) shows that this is not the case for Q = 16 µl/min and larger separation height spacing, where the peak heat transfer coefficient increases monotonically with increasing nozzle size, though the enhancement radius remains more or less constant.

#### 4.2.1 Peak Heat Transfer Enhancement

Fig. 9(d), (e) and (f) demonstrate the effect that varying the nozzle size has on the peak heat transfer achievable by the electrospray relative to that of natural convection alone. From Fig. 9 (d) it can be seen that for the 2.5 mm separation height, the heat transfer coefficient is independent of nozzle size and only mildly sensitive to the flow rate. This trend is not consistent for increased separation height though. Fig. 9(f) illustrates that while the lower flow rates of 4 µl/min and 8µl/min are still largely indifferent to increasing nozzle size the 16 µl/min shows sensitivity.

For Q = 16 µl/min and H = 12.5mm it is seen that the 9.9 times increase in the nozzle diameter results in a subsequent increases the heat transfer enhancement of 89.3%. In further comparison across Fig. 9(d), (e) and (f), at a constant Q = 16 µl/min and H = 2.5 mm and 7.5 mm, the heat transfer enhancement increases by 2.7% and 44.93% respectively for the 9.9 times nozzle diameter increase. This shows that at Q = 16 µl/min the heat transfer enhancement is sensitive to increasing nozzle size, with sensitivity growing for increasing target separation height, H.

## 5. CONCLUSIONS

The experimental results show that ultra-low flow rate electrospray cooling can provide improved heat transfer for low heat flux applications. Achieving an optimal electrospraying condition is shown to be dependent on separation height and the cooling fluid flow rate, with dependency on nozzle size was observed for certain case. At lower separation heights and greater flow rates a *saturation point* was observed where a subsequent increase in the flow rate of the working fluid yields no increase in the peak heat transfer coefficient although the cooling profile is altered. In the case of greater separation heights and lower flow rates a *dispersion threshold* was noted where the working fluid becomes too dispersed while in transit to the target surface resulting in the finely created droplets evaporating before or on contact with the thermal exchange surface. The enhancement region was shown to be slightly sensitive to varying flow rate and separation height although the heat transfer cooling profile does change to a scalable degree. The peak heat transfer coefficient, cooling profile and enhancement region were all shown to be largely independent of the nozzle size except for higher flow rates and separation heights. These results are of great importance for future work in defining an appropriate characteristic length and creating correlations in optimizing the application of single source electrosprays

## 6. ACKNOWLEDGEMENTS

This work was funded in part by an EU FP7 Marie Curie grant (FP7-PEOPLE-2009-IAPP: 251349-TaylorMed). The authors also gratefully acknowledge the Irish Research Council for their support during this research project. Thanks must also be given to Gerry Byrne of the Department of Mechanical and Manufacturing Engineering, Trinity College Dublin and Profector Life Sciences Ltd.

## 7. REFERENCES

1. Zeleny, J., *Instability of Electrified Liquid Surfaces.* Physical Review, 1917. **10**(1): p. 1-6.
2. Cloupeau, M. and B. Prunet-Foch, *Electrohydrodynamic spraying functioning modes: a critical review.* Journal of Aerosol Science, 1994. **25**(6): p. 1021-1036.
3. Deng, W. and A. Gomez, *The role of electric charge in microdroplets impacting on conducting surfaces.* Physics of Fluids, 2010. **22**(5): p. 1-4.
4. Feng, X. and J.E. Bryan, *Application of*

*electrohydrodynamic atomization to two-phase impingement heat transfer.* Journal of Heat Transfer, 2008. **130**(7).

5. Deng, W. and A. Gomez, *Electrospray cooling for microelectronics*. International Journal of Heat and Mass Transfer, 2011. **54**(11-12): p. 2270-2275.
6. Wang, H.C. and A.V. Mamishev, *Heat transfer correlation models for electrospray evaporative cooling chambers of different geometry types*. Applied Thermal Engineering, 2012. **40**: p. 91-101.
7. Hsiu-Che, W. and A.V. Mamishev. *Optimal heat transfer performance of the microfluidic electrospray cooling devices.* in *Semiconductor Thermal Measurement and Management Symposium (SEMI-THERM), 2011 27th Annual IEEE*. 2011.
8. Taylor, G., *Disintegration of Water Drops in an Electric Field.* Proceedings of the Royal Society of London. Series A, Mathematical and Physical Sciences, 1964. **280**(1382): p. 383-397.
9. Jaworek, A. and A. Krupa, *Classification of the modes of EHD spraying.* Journal of Aerosol Science, 1999. **30**(7): p. 873-893.
10. Eyring, C.F., S.S. Mackeown, and R.A. Millikan, *Fields Currents from Points.* Physical Review, 1928. **31**(5): p. 900-909.